

## 4. ESTIMATION OF SURFACE CHARACTERISTICS

### 4.1 The problem : separating roughness and moisture dependence

### 4.2 Model based moisture and surface roughness estimation

#### 4.2.1.1 Inverting Oh-Model

The inversion of the Oh-Model is based on the solution of relations introduced in the former paragraph. In the absence of an analytic solution,  $ks$  and  $\varepsilon'$  have to be estimated by an iterative procedure. In a first step,  $\Gamma^0$  is evaluated from

$$\left(\frac{2\theta}{\pi}\right)^{\frac{1}{\Gamma^0}} \left[ 1 - \frac{q}{0.23\sqrt{\Gamma^0}} \right] + \sqrt{p-1} = 0 \quad (1)$$

Using the measured co- and cross-polarised ratios,  $\Gamma^0$  can be estimated from (1) using an iterative technique. In this study, the Newton iteration approach was applied. Accordingly, the  $n$ -th Newton iteration for  $\Gamma^0$  is given by

$$x_n = \frac{a \frac{(x_{n-1})^2}{3} (1-b \cdot x_{n-1}) + c}{\left[ \frac{2 \cdot x_{n-1}}{3} \cdot \ln(a) \cdot (1-b \cdot x_{n-1}) - b \right] a \frac{(x_{n-1})^2}{3}} \quad (2)$$

Where

$$x := \frac{1}{\sqrt{\Gamma^0}}, \quad a := \frac{2\theta}{\pi}, \quad b := \frac{q}{0.23}, \quad c := \sqrt{p-1} \quad (3)$$

In a second step, from the approximated value  $x := \frac{1}{\sqrt{\Gamma^0}}$ ,  $\Gamma^0$  is extracted as  $\Gamma^0 = \left(\frac{1}{x_n}\right)^2$  and used to retrieve directly from Eq. (11.26) the real part of the dielectric constant

$$\varepsilon' = \left| \frac{1 + \sqrt{\Gamma^0}}{1 - \sqrt{\Gamma^0}} \right| \quad (4)$$

The obtained values for  $\varepsilon'$  are converted into  $m_v$  values after TOPP *et al.* (1980). Finally,  $\Gamma^0$  is used again in Eq. (11.58) to derive the surface roughness value  $ks$  as

$$k_s = \ln \left( \frac{(\sqrt{p} + 1)}{\left(\frac{2\theta}{\pi}\right)^{\frac{1}{3\Gamma^0}}} \right) \quad (5)$$

The iterative procedure converges rather slowly after about 30 iterations.

#### 4.2.1.2 Inverting Dubois-Model

The inversion of the empirical algorithm addressed by DUBOIS *et al.*(1995) is much simpler than the inversion of the model proposed by OH *et al.*(1992). Both, dielectric constant as well as surface roughness, can be retrieved directly from the model using the co-polarised backscatter coefficient and the local incidence angle by using the following two step inversion algorithm.

The first step is to retrieve the dielectric constant as

$$\varepsilon' = \frac{\left( \log_{10} \left( \frac{(\sigma_{HH}^0)^{0.7857}}{\sigma_{VV}^0} \right) 10^{-0.19} \cos^{1.82} \theta \sin^{0.93} \theta \lambda^{0.15} \right)}{-0.024 \tan \theta} \quad (6)$$

and using the estimated dielectric constant, in the second step, to retrieve the surface roughness

$$k_s = \sigma_{HH}^0{}^{1/1.4} 10^{2.75/1.4} \frac{\sin^{2.57} \theta}{\cos^{1.07} \theta} 10^{-0.02 \cdot \varepsilon' \cdot \tan \theta} \lambda^{-0.5} \quad (7)$$

As latter experiments demonstrated, the algorithm is performing relatively well also over sparsely vegetated areas at least at lower frequencies. For the discrimination of vegetated areas the  $\sigma_{VH}^0 / \sigma_{VV}^0$  ratio may be used as a good vegetation indication. Ratio values of  $\sigma_{VH}^0 / \sigma_{VV}^0 > -11$  dB indicate the presence of vegetation, and such areas are masked out and remain unconsidered by the inversion. As very well pointed out in DUBOIS *et al.* (1995); this condition leads to mask out also very rough surfaces, ( $k_s > 3$ ), which are mistaken for vegetated areas. Anyway, such fields are too rough to be accounted for by the model and have to be excluded.

The algorithm was applied only on areas where  $\sigma_{HH}^0 / \sigma_{VV}^0 < 1$  and  $\sigma_{VH}^0 / \sigma_{VV}^0 < -11$  dB in order to consider only areas lying within the validity range of the model. Also here, for the estimation of the soil moisture content the polynomial relation TOPP *et al.* (1980) for the conversion from  $\varepsilon'$  to  $m_v$  is used.

#### 4.2.1.3 Inverting the SPM model

The inversion of  $m_v$  by means of the SPM is straightforward: The formation of the  $R_s / R_p$  ratio leads directly to a non-linear equation, which for a given incidence angle, depends only on  $\varepsilon_r$ . Resolving for  $\varepsilon_r$  and converting it to  $m_v$ , it leads to the desired estimation of the soil moisture content.

#### 4.2.1.4 Inverting the X-Bragg model

##### ***Surface Roughness Estimation***

From Eq. (11.50), the polarimetric coherence between the Left-Left and Right-Right circular polarisations follows as (Mattia et al. 2000)

$$\gamma_{LLRR} := \frac{T_{22} - T_{33}}{T_{22} + T_{33}} = \text{sinc}(4\beta_1) \quad (8)$$

and depends only on the surface roughness. This is in accordance with the experimental observations reported in (Cloude et al. 1999). On the other hand, the anisotropy  $A$  can be interpreted as a generalised rotation invariant expression for  $\gamma_{LLRR}$ . Thus, the anisotropy is also expected to be independent of the dielectric properties of the surface.

Indeed, with increasing  $\beta_1$  the anisotropy falls monotonically from one to zero independent from the dielectric constant (and incidence angle) as shown in **Figure 1**. For  $ks$  values up to 1, i.e. up to  $\beta_1 = 90^\circ$ , an almost linear relation between  $A$  and  $ks$  is given, which is independent of the dielectric constant, and hence of the soil moisture content. Finally, above  $ks = 1$ ,  $A$  becomes insensitive to a further increase of roughness. This allows a straightforward separation of roughness from moisture estimation and represents one of the major advantages of the proposed model. Note that this result is independent of the choice of slope distribution. The form of  $P(\beta)$  affects only the mathematical expression of the anisotropy.

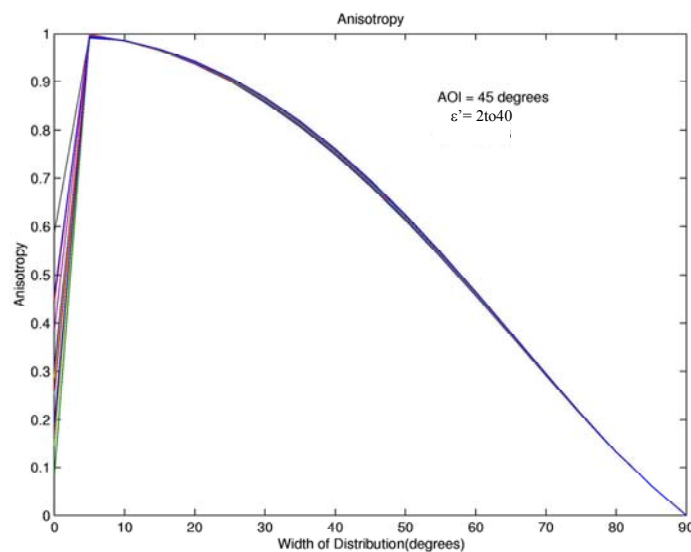


**Figure 1** Anisotropy as a function of the  $\beta_1$  parameter.

##### ***Soil Moisture Estimation***

Further structure in the expression of the perturbed coherency matrix, can be exposed, by plotting the entropy/alpha loci of points for different dielectric constant  $\epsilon'$  values and widths of slope distribution  $\beta_1$  for a local incidence angle  $\theta$  of 45 degree as shown in **Figure 1**. The loci are best interpreted in a polar co-ordinate system centred on the origin ( $H = 0, \alpha = 0$ ). In this sense, the radial co-ordinate corresponds to the dielectric constant while the azimuthal angle represents changes in roughness.

In the limit of a smooth surface, the entropy becomes zero and the alpha angle corresponds directly to the dielectric constant. However, as the entropy increases with increasing roughness, the apparent alpha angle value decreases, leading to an underestimation of the dielectric constant. Using the expression of the perturbed coherency matrix, it is possible to compensate this roughness induced underestimation of the alpha angle by tracking the loci of constant  $\epsilon'$  back to the  $H = 0$  line. In this way both the entropy and alpha value are required in order to obtain a corrected estimate of the surface moisture content, independent of the surface roughness estimation. The effect of the incidence angle on the alpha angle is shown in **Figure 2**. With increasing incidence angle from 10-50 degree, not only the alpha angle but also the corresponding entropy values increases. The reason for the raising entropy is the roughness induced increasing of cross polarised backscattered power and depolarisation.

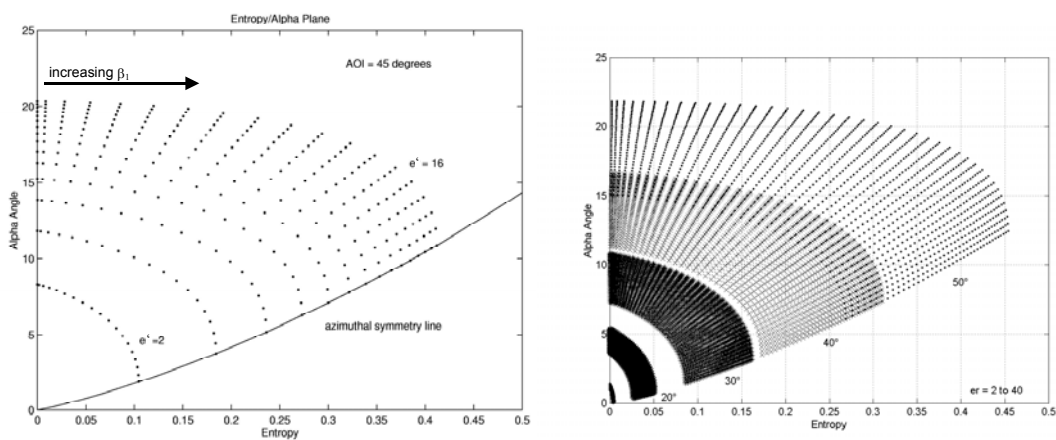


**Figure 2** The entropy/alpha plot for different dielectric constant and different local incidence angles.

Finally, the independence of  $A$  on soil moisture content and incidence angle is demonstrated once more in **Figure 3**. The anisotropy, which is a measure for the surface roughness, remain constant with changing dielectric constant and local incidence angle, providing the basis for decoupling roughness from moisture effects. Hence, by estimating three parameters, the entropy  $H$ , the anisotropy  $A$  and the alpha angle  $\alpha$ , we obtain a separation of roughness from surface dielectric constant. The roughness inversion is then performed directly from  $A$ , while the dielectric constant estimation arises from using combined  $H$  and  $\alpha$  values.

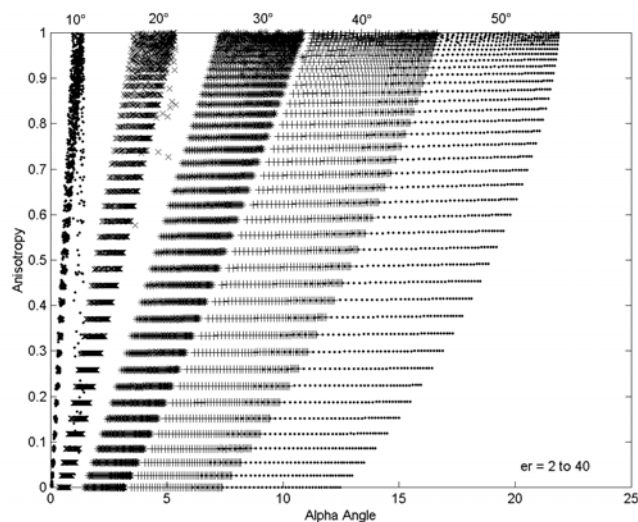


**Figure 3** Anisotropy as a function of the alpha angle

### 4.3 The problem : vegetation cover

The main limitation for surface parameter estimation from polarimetric SAR data is the presence of vegetation. This combined with the fact that most natural surfaces are temporarily or permanently covered by vegetation restricts significantly the importance of radar remote sensing for a wide spectrum of geophysical and environmental applications. However, the evolution of radar technology and techniques allows optimism concerning the vitiating of this limitation.

### 4.4 How to compensate vegetation effects

In the following two main approaches are proposed, the target decomposition as a pre-processing step to filter the vegetation effects out and the polarimetric SAR interferometry to separate the vegetation layer from the surface component in order to estimate the surface parameters under the vegetation cover.

#### 4.4.1 Using Polarimetry : Target Decomposition theory

The main objective of scattering decomposition approaches is to break down the polarimetric backscattering signature of a distributed scatterer – which is in general given by the superposition of different scattering contributions inside the resolution cell - into a sum of elementary scattering contributions related to single scattering processes. In general, scattering decompositions are rendered into two classes:

- The first class includes decompositions performed on the scattering matrix. In this case the received scattering matrix is expressed as the coherent sum of elementary scattering matrices, each related to a single scattering mechanism. Thus, scattering matrix decompositions are often referred in the literature as coherent decompositions. The most common scattering matrix decompositions are the decomposition into the Pauli scattering matrices and the Sphere-Diplane-Helix decomposition first proposed by E. KROGAGER in 1993, and further considered in KROGAGER & BOERNER 1996.
- The second class of decompositions contains decompositions performed on second order scattering matrices. Decompositions of the coherency (or covariance) matrix belong to this class. Such approaches decompose the coherency matrix of a distributed scatterer as the incoherent sum of three coherency matrices corresponding to three elementary orthogonal scattering mechanisms. The decomposition can be addressed, based on a scattering model or on physical requirements, on obtained scattering components, as for example their statistical independence.

An extended review of scattering decomposition approaches can be found in CLOUDE & POTTIER (1996).

Scattering decompositions are widely applied for interpretation, classification, and segmentation of polarimetric data (CLOUDE & POTTIER 1998, LEE *et al.* 1999). They have also been applied for scattering parameter inversion. In the following, their application in the context of surface parameter estimation is considered. Due to the fact that natural surfaces are distributed scatterers, coherency matrix decompositions are more suited for surface scattering problems than scattering matrix decomposition approaches, and therefore, only such approaches will be treated next.

#### 4.4.1.1 Freeman/Durden approach

- A. FREEMAN developed from 1992 to 1998 a three-component scattering model suited for classification and inversion of air- and space-borne polarimetric SAR image data. His decomposition approach belongs to the class of model-based decompositions and uses simple scattering processes to model the scattering behaviour of vegetated terrain. According to this model, backscattering from vegetated terrain can be regarded as the superposition of three single scattering processes: surface scattering, dihedral scattering and volume scattering. Assuming the three processes to be independent from one another, each contributes to the total observed coherency matrix  $[T]$  as

$$[T] = [T_S] + [T_D] + [T_V] \quad (9)$$

where  $[T_S]$  is the coherency matrix for the surface scattering,  $[T_D]$  the dihedral scattering, and  $[T_V]$  for the volume scattering contribution, respectively.

#### **Surface Scattering Contribution**

The first scattering contribution is the surface scattering modelled by a Bragg scatterer (see **Figure 4**) with a scattering matrix and a Pauli scattering vector given by

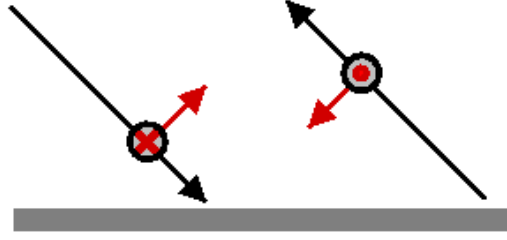


**Figure 4** Bragg scattering mechanism

$$[S_S] = \begin{bmatrix} R_S & 0 \\ 0 & R_P \end{bmatrix} \rightarrow \bar{k}_S = [R_S + R_P, R_P - R_S, 0]^T \quad (10)$$

where  $R_S$  is the perpendicular and  $R_P$  the vertical to the scattering plane Bragg coefficient

$$R_S = \frac{\cos \theta - \sqrt{\varepsilon_r - \sin^2 \theta}}{\cos \theta + \sqrt{\varepsilon_r - \sin^2 \theta}} \quad R_P = \frac{(\varepsilon_r - 1)(\sin^2 \theta - \varepsilon_r(1 + \sin^2 \theta))}{(\varepsilon_r \cos \theta + \sqrt{\varepsilon_r - \sin^2 \theta})^2} \quad (11)$$

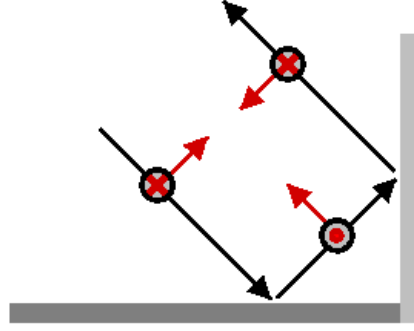
and  $\varepsilon_r$  the dielectric constant of the surface. The scattering vector of (11) leads to a coherency matrix of the form

$$[T_S] = f_S \begin{bmatrix} \beta^2 & \beta & 0 \\ \beta & 1 & 0 \\ 0 & 0 & 0 \end{bmatrix} \quad (12)$$

Accordingly, the surface contribution is described by two parameters: the real ratio  $\beta = \frac{R_S + R_P}{R_S - R_P}$  and the backscattering contribution  $f_S = |R_S - R_P|^2$ .

### Dihedral Scattering Contribution

The second scattering mechanism considered by the model is anisotropic dihedral scattering. The scattering matrix of a dihedral scatterer can be expressed as the product of the two scattering matrices describing the forward scattering event occurring at each of the two planes of the dihedral. The model assumes the dihedral to be formed by two orthogonal Bragg scattering planes with the same or different dielectric properties. In this case, the scattering is completely described by the Fresnel reflection coefficients of each reflection plane. For example, the scattering matrix of a soil-trunk dihedral interaction is obtained as


**Figure 5** Dihedral scattering mechanism

$$[S_D] = \begin{bmatrix} 1 & 0 \\ 0 & -1 \end{bmatrix} \begin{bmatrix} 1 & 0 \\ 0 & e^{i\varphi} \end{bmatrix} \begin{bmatrix} R_{SS} & 0 \\ 0 & R_{PS} \end{bmatrix} \begin{bmatrix} R_{ST} & 0 \\ 0 & R_{PT} \end{bmatrix} = \begin{bmatrix} R_{SS}R_{ST} & 0 \\ 0 & -R_{PS}R_{PT}e^{i\varphi} \end{bmatrix} \quad (13)$$

The third matrix describes the first forward reflexion at the soil.  $R_{SS}$  is the perpendicular and  $R_{PS}$  the parallel to the reflection plane Fresnel reflection coefficient for the soil scatterer

$$R_{SS} = \frac{\cos\theta - \sqrt{\varepsilon_S - \sin^2\theta}}{\cos\theta + \sqrt{\varepsilon_S - \sin^2\theta}} \quad \text{and} \quad R_{PS} = \frac{\varepsilon_S \cos\theta - \sqrt{\varepsilon_S - \sin^2\theta}}{\varepsilon_S \cos\theta + \sqrt{\varepsilon_S - \sin^2\theta}} \quad (14)$$

and  $\varepsilon_S$  is the dielectric constant of the soil. The fourth matrix describes the second forward reflection at the trunk, with  $R_{ST}$  the perpendicular and  $R_{PT}$  the parallel Fresnel reflection coefficient for the trunk scatterer

$$R_{ST} = \frac{\cos\theta - \sqrt{\varepsilon_T - \sin^2\theta}}{\cos\theta + \sqrt{\varepsilon_T - \sin^2\theta}} \quad \text{and} \quad R_{PT} = \frac{\varepsilon_T \cos\theta - \sqrt{\varepsilon_T - \sin^2\theta}}{\varepsilon_T \cos\theta + \sqrt{\varepsilon_T - \sin^2\theta}} \quad (15)$$

$\varepsilon_T$  the dielectric constant of the trunk. The second matrix accounts for any differential phase  $\varphi$  between HH and VV incorporated by propagation through the vegetation or scattering. Finally, the first matrix performs the transformation from the forward- to the backscattering geometry. The corresponding Pauli scattering vector, follows from (15) as

$$\vec{k}_D = [R_{SS}R_{ST} - R_{PS}R_{PT}e^{i\varphi}, R_{SS}R_{ST} + R_{PS}R_{PT}e^{i\varphi}, 0]^T \quad (16)$$

leading to a coherency matrix of the form

$$[T_D] = f_D \begin{bmatrix} \alpha^2 & -\alpha & 0 \\ -\alpha & 1 & 0 \\ 0 & 0 & 0 \end{bmatrix} \quad (17)$$

Thus, the dihedral contribution is described by the complex ratio  $\alpha = \frac{R_{SS}R_{ST} - R_{PS}R_{PT}e^{i\varphi}}{R_{SS}R_{ST} + R_{PS}R_{PT}e^{i\varphi}}$ ,

and, by the real backscattering amplitude  $f_D = |R_{SS}R_{ST} + R_{PS}R_{PT}e^{i\varphi}|^2$ .



### Volume Scattering Contribution

The third scattering component of the model is a randomly oriented volume of dipoles. The starting point for the evaluation of the corresponding coherency matrix is the scattering matrix of a horizontally oriented dipole

$$[S] = m \begin{bmatrix} 1 & 0 \\ 0 & 0 \end{bmatrix} \quad (18)$$

where  $m$  is the dipole backscattering amplitude. The scattering matrix obtained by rotating the dipole by an angle of  $\theta$  about the line-of-sight may be written as

$$[S(\theta)] = \begin{bmatrix} \cos \theta & \sin \theta \\ -\sin \theta & \cos \theta \end{bmatrix} \begin{bmatrix} m & 0 \\ 0 & 0 \end{bmatrix} \begin{bmatrix} \cos \theta & -\sin \theta \\ \sin \theta & \cos \theta \end{bmatrix} = m \begin{bmatrix} \cos^2 \theta & \cos \theta \sin \theta \\ \cos \theta \sin \theta & \sin^2 \theta \end{bmatrix} \quad (19)$$

and the corresponding Pauli scattering vector is given by

$$\vec{k}_p(\theta) = [\cos^2 \theta + \sin^2 \theta, \cos^2 \theta - \sin^2 \theta, 2 \cos \theta \sin \theta]^T \quad (20)$$

The coherency matrix of a volume of such dipoles is now obtained by averaging the outer product of the scattering vector, as given in (20), over the orientation distribution of the dipoles in the volume

$$[T_V] = \int_0^{2\pi} \vec{k}_p(\theta) \cdot \vec{k}_p^+(\theta) P(\theta) d\theta \quad (21)$$

where  $P(\theta)$  is the probability density function of the orientation angle distribution of the dipoles in the volume.

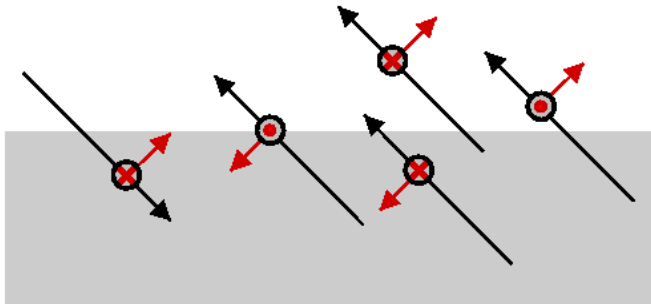


**Figure 6** . Volume scattering mechanism

As the volume is assumed to be uniformly randomly oriented,  $P(\theta) = 1/(2\pi)$ , and from (21) follows

$$[T_V] = f_V \begin{bmatrix} 2 & 0 & 0 \\ 0 & 1 & 0 \\ 0 & 0 & 1 \end{bmatrix} \quad (22)$$

Consequently, the random volume contribution is described by a single parameter, namely its backscattering amplitude  $f_V$ . Assuming the three scattering processes to be independent from each other, the total coherency matrix is obtained by the superposition of the three corresponding coherency matrices as

$$[T] = f_s \begin{bmatrix} \beta^2 & \beta & 0 \\ \beta & 1 & 0 \\ 0 & 0 & 0 \end{bmatrix} + f_D \begin{bmatrix} \alpha^2 & -\alpha & 0 \\ -\alpha & 1 & 0 \\ 0 & 0 & 0 \end{bmatrix} + f_V \begin{bmatrix} 2 & 0 & 0 \\ 0 & 1 & 0 \\ 0 & 0 & 1 \end{bmatrix} \rightarrow \quad (23)$$

$$[T] = \begin{bmatrix} f_s \beta^2 + f_D \alpha^2 + 2f_V & f_s \beta - f_D \alpha & 0 \\ f_s \beta - f_D \alpha & f_s + f_D + f_V & 0 \\ 0 & 0 & f_V \end{bmatrix} \quad (24)$$

Tab. 2 summarises the scattering contributions for the individual elements of the obtained coherency matrix  $[T]$ . The correlations  $\langle (S_{HH} + S_{VV})S_{HV}^* \rangle$  and  $\langle (S_{HH} - S_{VV})S_{HV}^* \rangle$  vanish as a consequence of the reflection symmetry of all contributions.

Elements of $[T]$	Surface Scattering	Double Bounce Scattering	Volume Scattering
$ S_{HH} + S_{VV} ^2$	$f_s \beta^2$ +	$f_D  \alpha ^2$	+ $f_V$
$ S_{HV} ^2$	0 +	0	+ $f_V/3$
$ S_{HH} - S_{VV} ^2$	$f_s$ +	$f_D$	+ $f_V$
$(S_{HH} + S_{VV})(S_{HH} - S_{VV})^*$	$f_s \beta$ -	$f_D \alpha$	+ $f_V$

Tab. 2: Scattering contributions for the individual elements of  $[T]$ .

Eq. (11.74) describes the scattering process in terms of five parameters: The three scattering contributions  $f_s$ ,  $f_D$ , and,  $f_V$  which are real and positive quantities, the complex coefficient  $\alpha$  and the real coefficient  $\beta$ . On the other hand, there are only three real and one complex equations available (obtained from the  $(|S_{HH} + S_{VV}|^2, |S_{HH} - S_{VV}|^2, |S_{HV}|^2, \text{ and } (S_{HH} + S_{VV})(S_{HH} - S_{VV})^*$  elements of  $[T]$  respectively) to resolve for the five parameters. Therefore, one of the model parameters has to be fixed. In the case for which the surface contribution is stronger than the dihedral one,  $\alpha$  is fixed to be equal 1, while in the opposite case, for which the dihedral contribution is stronger than the surface one,  $\beta$  is fixed to be equal 1. Which of both contributions is stronger is decided according to following empirical rule (VAN ZYL 1992)

$$\begin{aligned} \text{If } f_s \beta > f_D \alpha & \rightarrow \text{Dominant Surface Scattering} \rightarrow \beta = 1 \\ \text{If } f_s \beta < f_D \alpha & \rightarrow \text{Dominant Dihedral Scattering} \rightarrow \alpha = 1 \end{aligned}$$

Note that, neither the surface scattering nor the dihedral scattering mechanism are contributing to the  $|S_{HV}|^2$  term. Thus this term is used to estimate directly the volume scattering contribution which is then subtracted from the  $|S_{HH} + S_{VV}|^2, |S_{HH} - S_{VV}|^2$  and  $(S_{HH} + S_{VV})(S_{HH} - S_{VV})^*$  terms in order to extract the parameters for the surface and dihedral contributions.

#### 4.4.1.2 Eigenvalue : Entropy/Alpha approach

In this Section, the polarimetric eigenvector decomposition of the coherency matrix is introduced as a pre-filtering technique, which can be applied on the experimental data in order to improve the performance of the inversion algorithms. The coherency matrix  $[T]$  is obtained from an ensemble of scattering matrix samples  $[S_i]$  by forming the Pauli scattering vectors

$$[S_i] = \begin{bmatrix} S_{HH} & S_{HV} \\ S_{VH} & S_{VV} \end{bmatrix} \rightarrow \bar{k}_{P_i} = \frac{1}{\sqrt{2}} [S_{HH} + S_{VV}, S_{HH} - S_{VV}, 2S_{HV}]^T \quad (25)$$

Averaging the outer product of them over the given samples, yields

$$[T] := \langle \bar{k}_{P_i} \cdot \bar{k}_{P_i}^+ \rangle = \begin{bmatrix} \langle |S_{HH} + S_{VV}|^2 \rangle & \langle (S_{HH} + S_{VV})(S_{HH} - S_{VV})^* \rangle & 2\langle (S_{HH} + S_{VV})S_{HV}^* \rangle \\ \langle (S_{HH} - S_{VV})(S_{HH} + S_{VV})^* \rangle & \langle |S_{HH} - S_{VV}|^2 \rangle & 2\langle (S_{HH} - S_{VV})S_{HV}^* \rangle \\ 2\langle S_{HV}(S_{HH} + S_{VV})^* \rangle & 2\langle S_{HV}(S_{HH} - S_{VV})^* \rangle & 4\langle |S_{HV}|^2 \rangle \end{bmatrix} \quad (26)$$

Since the coherency matrix  $[T]$  is by definition hermitian positive semi-definite, it can always be diagonalised by an unitary similarity transformation of the form

$$[T] = [U_3][\Lambda][U_3]^{-1} \text{ where } [\Lambda] = \begin{bmatrix} \lambda_1 & 0 & 0 \\ 0 & \lambda_2 & 0 \\ 0 & 0 & \lambda_3 \end{bmatrix}, \text{ and } [U_3] = \begin{bmatrix} | & | & | \\ \bar{e}_1 & \bar{e}_2 & \bar{e}_3 \\ | & | & | \end{bmatrix}. \quad (27)$$

$[\Lambda]$  is the diagonal eigenvalue matrix with elements of the real non-negative eigenvalues of  $[T]$ ,  $0 \leq \lambda_3 \leq \lambda_2 \leq \lambda_1$ , and  $[U_3]$  is a special unitary matrix with the corresponding orthonormal eigenvectors  $\bar{e}_i$ . The idea of the eigenvector approach is to use the diagonalisation of  $[T]$  obtained from a partial scatterer, which is in general of rank 3, in order to represent it as the non-coherent sum of three deterministic orthogonal scattering mechanisms. Each of the three scattering contributions, expressed in terms of a coherency matrices  $[T_1]$ ,  $[T_2]$ , and  $[T_3]$ , is obtained from the outer product of one eigenvector and weighted by its appropriate eigenvalue.

$$[T] = \lambda_1(\bar{e}_1 \cdot \bar{e}_1^+) + \lambda_2(\bar{e}_2 \cdot \bar{e}_2^+) + \lambda_3(\bar{e}_3 \cdot \bar{e}_3^+) = [T_1] + [T_2] + [T_3] \quad (28)$$

$[T_1]$ ,  $[T_2]$ , and  $[T_3]$ , are rank one coherency matrices, i.e., they represent deterministic non-depolarising scattering processes and correspond therefore to a single scattering matrix. Furthermore, as they are built up from the orthonormal eigenvectors of  $[T]$ , they are statistically independent from each other

$$[T] = \begin{bmatrix} t_1 & t_2 & t_3 \\ t_2^* & t_4 & t_5 \\ t_3^* & t_5^* & t_6 \end{bmatrix} = \begin{bmatrix} t_{11} & t_{12} & t_{13} \\ t_{12}^* & t_{14} & t_{15} \\ t_{13}^* & t_{15}^* & t_{16} \end{bmatrix} + \begin{bmatrix} t_{21} & t_{22} & t_{23} \\ t_{22}^* & t_{24} & t_{25} \\ t_{23}^* & t_{25}^* & t_{26} \end{bmatrix} + \begin{bmatrix} t_{31} & t_{32} & t_{33} \\ t_{32}^* & t_{34} & t_{35} \\ t_{33}^* & t_{35}^* & t_{36} \end{bmatrix} \quad (29)$$

According to a simplified interpretation, for natural surface scatterers the first scattering component  $[T_1]$  represents the dominant anisotropic surface scattering contribution. The second and third components,  $[T_2]$  and  $[T_3]$ , represent secondary dihedral and/or multiple scattering contributions, respectively. In this sense, disturbing secondary scattering effects biasing the original scattering amplitudes can be filtered out by applying the eigenvector decomposition of (28) and omitting one or both secondary contributions for the inversion of the surface parameters.

There are some important differences between the two decompositions. The first one deals with the statistical independence of the obtained components. While the eigenvector decomposition leads to three rank 1 components, which are orthogonal to each other (i.e. statistically independent), the scattering components of the model-based decomposition are not independent. On the one hand, the surface and the dihedral component are non-

depolarising rank 1 scatterers independent from each other. But on the other hand, the volume component has a rank 3 coherency matrix corresponding to a depolarising scatterer present in all polarisations. Further, according to the model based decomposition, cross-polarisation is generated only by depolarisation. For cross-polarisation induced by rotation about the line-of-sight, caused for example by terrain slopes, is not accounted for. Hence, any amount of correlated cross-polarisation becomes misinterpreted as volume scattering contribution. In contrast, due to the statistical independence of the obtained components, the eigenvector decomposition, is able to distinguish correlated from uncorrelated contributions in the polarimetric channels. Finally, while the scattering contributions of the eigenvector decomposition are invariant under line-of-sight rotations, as a consequence of the eigenvector invariance under unitary transformations, the scattering contributions obtained from the model based decomposition are not.

#### 4.4.2 Polarimetric SAR Interferometry

One often proposed approach for solving the problem of surface parameter inversion under vegetation cover is to use longer wavelengths (lower frequencies). P-band is for example such a potential frequency candidate with sufficient high penetration into and through vegetation layers. However, first experimental results at P-band indicate that this approach solves only one part of the problem. In the case of dense vegetation the efficient separation of vegetation scattering from surface scattering contributions - required for the extraction of the underlying surface characteristics - is not possible. Furthermore, the fact that the effective roughness is scaled by the wavelength makes moderate rough bare surfaces to appear very smooth at P-band, implying low backscattering coefficients often close to the system noise floor (HAJNSEK *et al.* 2001). In this case, additive noise becomes a significant limitation. Thus, single frequency and conventional polarimetry alone seems to be unable to resolve satisfactory the problem. More promising appears the option of dual frequency (for example L- and P-band) fully polarimetric configurations (MOGHADDAM & SAATCHI 2000). The combination of two or more frequencies promises on the one hand the coverage of a wider class of natural surface conditions and on the other hand more robust estimates. However, a note of caution is required: A changing of wavelength may also imply a change of the scattering process, and affects the applicability of the inversion algorithms (HAJNSEK *et al.* 2001).

The second challenging way is the new technique of polarimetric interferometry (CLOUDE & PAPATHANASSIOU 1998, PAPATHANASSIOU & CLOUDE 1999, PAPATHANASSIOU and CLOUDE 2000). The sensitivity of the interferometric phase plus coherence to the location of the effective scattering center inside the resolution cell, combined with the strong influence of ground scattering on the location of the scattering-center, provides for the first time a sensible way to estimate even weak ground scattering under vegetation. Additionally, the variation of the interferometric coherence as a function of baseline allows conclusions about the vegetation layer over the surface. On the other hand, polarimetry is important for the inversion of the surface scattering problem. Thus, the combination of polarimetry and interferometry, in terms of polarimetric interferometry, has a very promising application for the extraction of surface information under vegetation.

In Part II of the tutorial the principles of polarimetric SAR interferometry technique are presented in detail.

## 4.5 Do it yourself

- Using simulated POLSAR data for vegetated and bare surfaces to estimate roughness and moisture content

## 4.6 References

- ANTOKOL'SKII, M. L., Reflection of waves from a perfectly reflecting rough surface, DAN SSSR, vol. 62, pp. 203-206, 1948.
- BASS, F. G. & FUKS, I. M., 'Wave Scattering from Statistically Rough Surfaces', *International Series in Natural Philosophy*, vol. 93, p. 525, 1979.
- BEAUDOIN, A. LE TOAN, T. & GWYN, Q. H. J., 'SAR observations and modelling of the C-band backscatter variability due to multi scale geometry and soil moisture', *IEEE Transactions on Geoscience and Remote Sensing*, vol. 28, no. 5, pp. 886-895, 1990.
- BECKMANN, P. & SPIZZICHINO A., 'The Scattering of Electromagnetic Waves from Rough Surfaces', Oxford: Pergamon, Reprinted 1978 by Artech House Inc., Norwood, Massachusetts, USA, p. 503, 1963.
- BOERNER, W.-M. *et al.*, 'Polarimetry in Radar Remote Sensing: Basic and Applied Concepts', Chapter 5 in F. M. Henderson and A.J. Lewis (ed.), 'Principles and Applications of Imaging Radar', vol. 2 of Manual of Remote Sensing, (ed. R. A. Reyerson), Third Edition, John Wiley & Sons, New York, 1998.
- Borgeaud, M. & Noll, J., '*Analysis of Theoretical Surface Scattering Models for Polarimetric Microwave Remote Sensing of Bare Soils*', *International Journal of Remote Sensing*, vol. 15, no. 14, pp. 2931-2942, 1994.
- BREKHOVSKIH, L. M., 'Radio wave diffraction by a rough surface', DAN SSSR, vol. 79, no. 4, pp. 585-588, 1951.
- BURWELL, R. E., ALLMARAS, R. R. & AMEMIYA, M., 'A field measurement of total porosity and surface microrelief of soils', *J. of Soil Science*, vol. 34, pp. 577 – 597, 1963.
- CLOUDE, S. R. & POTTIER, E., 'A Review of Target Decomposition Theorems in Radar Polarimetry', *IEEE Transactions on Geoscience and Remote Sensing*, vol. 34, no. 2, pp. 498–518, 1996.
- CLOUDE, S. R. & POTTIER, E., 'An Entropy Based Classification Scheme for Land Applications of Polarimetric SAR', *IEEE Transactions on Geoscience and Remote Sensing*, vol. 35, no. 1, pp. 68-78, 1997.

- CLOUDE, S. R. & K. PAPATHANASSIOU, "Polarimetric SAR Interferometry", *IEEE Transactions on Geoscience and Remote Sensing*, vol. 36, pp. 1551-1565, Sep. 1998
- S.R. Cloude, K.P. Papathanassiou & E. Pottier, "Radar Polarimetry and Polarimetric Interferometry", *IEICE Transaction on Electronics*, vol. E84-C, no. 12, pp. 1814-1822, Dec.2001.
- Cloude, S. R., I. Hajnsek, & K. P. Papathanassiou, 'An Eigenvector Method for the Extraction of Surface Parameters in Polarimetric SAR', *Proceedings of the CEOS SAR Workshop*, Toulouse 1999, ESA SP-450, pp. 693 – 698, 1999.
- CHEN, M. F. & FUNG, A. K., 'A Numerical Study of the Regions of Validity of the Kirchhoff and Small-Perturbation Rough Scattering Models', *IEEE Transactions on Geoscience and Remote Sensing*, vol. 23, no. 2, pp. 163-170, 1988.
- CHEN, K.S., WU, T.D., TSAY, M.K. & FUNG, A. K., 'A Note on the Multiple Scattering in an IEM Model', *IEEE Transactions on Geoscience and Remote Sensing*, vol. 38, no. 1, pp. 249-256, 2000.
- CURRENCE, H. D. & W. G. LOVELY, 'An automatic soil surface profilometer', *Trans ASAE*, vol. 14, pp. 69-71, 1971.
- DALTON, F. N. & VAN GNEUCHTEN, M. Th., 'The TDR method for measuring soil water content and salinity', *Geoderma*, vol. 38, pp 237 – 250, 1986.
- DAVIES, H., 'The Reflection of electromagnetic waves from a rough surface', *Proceedings of IEEE*, Pt. 4, vol. 101, no. 7, pp. 209-214, 1954.
- DAVIDSON, M. W. J., LE TOAN, T., MATTIA, F., SATALINO, G., MANNINER, T. & BORGEAUD, M., 'On the characterisation of agricultural soil roughness for radar remote sensing studies', *IEEE Transactions on Geoscience and Remote Sensing*, vol. 38, no. 2, pp. 630-640, 2000.
- DE LOOR, G. P., 'The dielectric properties of wet materials', *Proceedings of IGARSS 82*, Muenchen, TP – 1, 1 – 5, 1982.
- DOBSON, M. C. ULABY, F. T., HALLIKAINEN, M. T. & EL-RAYES, M A., 'Microwave Dielectric Behaviour of Wet Soil – Part II: Empirical Models and Experimental Observations', *IEEE Transaction on Geoscience of Remote Sensing*, vol. 23, no. 1, pp. 35 – 46, 1985.
- DOOGE, J. C. I., 'Hydrology in perspective', *Hydrological Sciences Journal*, vol. 33, pp. 61-85, 1988.
- DUBOIS, P. C. VAN ZYL, J. J. & ENGMAN, T., 'Measuring Soil Moisture with Imaging Radars', *IEEE Transactions on Geoscience and Remote Sensing*, vol. 33, no. 4, pp. 916-926, 1995
- FEINBERG, E. L., Radio wave propagation along a real surface, *J. Phys. USSR*, vol. 8, pp. 317-330, 1944, vol. 9, pp. 1-6, 1945 and vol. 10, pp. 410-418, 1946
- FREEMAN, A. & DURDEN, S. L., 'A three-component scattering model to describe polarimetric SA Data', in *Proceedings SPIE Conference Radar Polarimetry*, San Diego, CA, pp. 213-224, 1992
- FREEMAN, A. & DURDEN, S. L., 'A Three-Component Scattering Model for Polarimetric SAR Data', *IEEE Transactions on Geoscience and Remote Sensing*, vol. 36, no. 3, pp. 963-973, 1998.

- FUNG, A. K., LI, Z. & CHEN, K. S., 'Backscattering from a randomly rough surface', *IEEE Transactions on Geoscience and Remote Sensing*, vol. 30, no. 2, pp. 356-369, 1992.
- FUNG, A. K., 'Microwave Scattering and Emission Models and their Applications', Arctech House Norwood USA, p. 573, 1994.
- GARDNER, W. H., 'Water content', in: *Methods of soil analysis, part 1*, 2<sup>nd</sup> edn., ed. A. Klute, *Agronomy*, vol. 9, pp. 493 – 544, 1986.
- Hajnsek, I., 'Inversion of Surface Parameters Using Polarimetric SAR', DLR-Science Report, vol. 30, ISSN 1434-8454, p. 224, 2001.
- Hajnsek, I., Papathanassiou, K. P. & Cloude, S. R., 'Surface Parameter Estimation Using fully polarimetric L- and P-band Radar data', *Proc. 3<sup>rd</sup> International Symposium, 'Retrieval of Bio-Geophysical Parameters from SAR Data for Land Applications'*, 11-14 Sept. 2001, Sheffield, UK, ESA SP-475, January 2002, pp. 159-164
- HAJNSEK, I., 'Pilotstudie Radarbefliegung der Elbaue', Endbericht TP. I.2, p. 93, 1999, in: *Verbundvorhaben Morphodynamik der Elbe, FKZ 0339566 des BMBF*, in: *Interner Bericht DLR 551-1/2001*.
- HAJNSEK, I., CLOUDE, S. R., LEE, J. S. & POTTIER, E., 'Terrain Correction for Quantitative Moisture and Roughness Retrieval Using Polarimetric SAR Data', *Proceedings IGARSS'00*, Honolulu, Hawaii, pp. 1307-1309, July 2000.
- HAJNSEK, I., POTTIER, E. & CLOUDE, S. R., 'Slope Correction for Soil Moisture and Surface Roughness Retrieval', *Proceedings of third European Conference on Synthetic Aperture Radar EUSAR 2000*, pp. 273-276, May 2000.
- HALLIKAINEN, M. T., ULABY, F. T., DOBSON, M. C., EL-RAYES, M A., & WU, L.-K., 'Microwave Dielectric Behaviour of Wet Soil – Part I: Empirical Models and Experimental Observations', *IEEE Transactions on Geoscience and Remote Sensing*, vol. 23, no. 1, pp. 25 – 33, 1985.
- HERKELRATH, W. N., HAMBURG, S. P. & MURPHY, F., 'Automatic, real-time monitoring of soil moisture in a remote field area with TDR', *Water Resour. Res.*, vol. 27, no. 5, pp. 857-864, 1991.
- HOLMES, J. W., TAYLOR, S. A., & RICHARDS, S. J., 'Measurement of soil water', in: *Irrigation of agricultural Lands*, eds. R.M. Hagan, H.R. Haise, and T.W. Edminster. *Agronomy*, no. 11, pp. 275 – 303, 1967.
- ISAKOVICH, M. A., 'Wave scattering from a statistically rough surface', *Otchet FIAN SSSR, Akustich. Lab.*, 1953, *Trudy Akust. in-ta AN SSSR*, no. V, pp. 152-251, 1969.
- ISHIMARU, A., 'Wave Propagation and Scattering in Random Media: Single Scattering and Transport Theory', vol. I, 'Multiple Scattering, Turbulence, Rough Surfaces and Remote Sensing', New York: Academic Press, 1978.
- JESCHCKE, W., 'Digital close-range photogrammetry for surface measurement', *IAPRS*, Zürich, vol. 28-5, pp. 1058-1065, 1990.
- KELLER, J. M., CROWNOVER, R. & CHEN, R., 'Characteristics of natural sciences related to the fractal dimension', *IEEE Trans. On Pattern Anal. And Mach. Intell.*, vol. 9, no. 5, 1987.
- KROGAGER, E., 'Aspects of Polarimetric Radar Imaging', Thesis Danish Defense Research Establishment, p. 235, 1993

- KROGAGER, E. & W.M. BOERNER, 'On the Importance of Utilizing Polarimetric Information in Radar Imaging Classification', *AGARD Proc.* 582-17, 1-13, April 1996.
- KUIPERS, H., 'A reliefmeter for soil cultivation studies', *Neth. J. of Agric. Sci.*, pp. 255-262, 1957.
- LEE, J. S., GRUNES, M. R., AINSWORTH, T. L., DU, L. J., SCHULER, D. L. & CLOUDE, S. R., 'Unsupervised Classification Using Polarimetric Decomposition and the Complex Wishart Classifier', *IEEE Transactions on Geoscience and Remote Sensing*, vol. 37, no. 5, pp. 2249 – 2258, 1999.
- LEE, J. S., D. L. SCHULER & T. L. AINSWORTH, 'Polarimetric SAR Data Compensation for Terrain Azimuth Slope Variation', *IEEE Transactions on Geoscience and Remote Sensing*, vol. 38, no. 5, part I, pp. 2153-2163, 2000.
- MANDEL'SHAM, L. I., 'Irregularities in a free liquid surface', *Poln. sobr. trudov* (collected works), vol. 1, pp. 246-260, 1948, first pub. as 'Über die Rauhgigkeit freier Flüssigkeitsoberflächen', *Ann. Physik*, vol. 41, no. 8, pp. 609-624, 1913.
- MARSHALL, T. J., HOLMES, J. W. & ROSE, C. W., 'Soil Physics', *Cambridge University Press*, third edition, p. 453, 1999.
- MARSHALL(A), T. J., 'The nature, development and significance of soil structure', *Trans. Int. Soc. Soil Sci.* Comm. IV and V, NZ, pp. 243-57, 1962(a).
- MATTIA, F. & LE TOAN, T., 'Backscattering properties of multi scale rough surfaces', *J. Electromagn. Waves Applicat.*, vol. 13, pp. 491-526, 1999.
- MATTIA, F., LE TOAN, T., SOUYRIS, J. C., DE CAROLIS, G., FLOURY, N., POSA, F. & PASQUARIELLO, G., 'The Effect of Surface Roughness on Multi-Frequency Polarimetric SAR data', *IEEE Transactions on Geoscience and Remote Sensing*, vol. 35, no. 4, pp. 954-965, 1997.
- OGILVY, J. A. & FOSTER, J. R., 'Rough surfaces: Gaussian or exponential statistics', *Phys. Rev. D: Appl. Phys.*, vol. 22, pp. 1243-1251, 1989.
- OH, Y., SARABANDI, K. & ULABY, F. T., 'An Empirical Model and an Inversion Technique for Radar Scattering from Bare Soil Surfaces', *IEEE Transactions on Geoscience and Remote Sensing*, vol.30, no. 2, pp. 370-381, 1992.
- PAPATHANASSIOU, K. P., "Polarimetric SAR Interferometry", *Dr.-Tech. Thesis*, TU Graz, 1999 February 25, DLR-FB 99-07, 1999
- PAPATHANASSIOU, K. P., CLOUDE, S. R. & REIGBER, A., 'Estimation of Vegetation Parameters using Polarimetric SAR Interferometry, Part I and Part II', *Proceedings of CEOS SAR Workshop 1999*, CNES, Toulouse, France, 26-29 October 1999.
- POTTIER, E., SCHULER, D. L., LEE, J.-S., & AINSWORTH, T. L., 'Estimation of the Terrain Surface Azimuthal/Range Slopes Using Polarimetric Decomposition of Polsar Data', *Proceeding IGARSS'1999*, Hamburg, pp. 2212-2214, 1999
- PRIETZSCH, C., 'Vergleichende Analyse von SAR-Daten für die Regionalisierung des Wassergehaltes im Oberboden', *Dissertation*, Mathematisch- Naturwissenschaftlichen Fakultät, Universität Potsdam, p.159, 1998.
- RAYLEIGH, LORD, 'The Theory of Sound', *Scientific Papers*, vol. 6 in 3, New York: Dover, 1964, first edition 1877.



- RICE, S. O., 'Reflection of electromagnetic waves from slightly rough surfaces', *Comm. Pure Appl. Math.*, vol. 4, no. 2/3, pp. 351-378, 1951.
- REIGBER, A.; MOREIRA A, "First demonstration of airborne SAR tomography using multibaseline L-band data", *IEEE Transactions on Geoscience and Remote Sensing*, Volume: 38 Issue: 5 Part: 1, Sept. 2000, Page(s): 2142 -2152
- ROTH, C. H., MALICKI, M. A. & PLAGGE, R., 'Empirical evaluation of the relationship between soil dielectric constant and volumetric water content as the basis for calibrating soil moisture measurements by TDR', *J. Soil. Sci.*, vol. 43, pp. 1 – 13, 1992.
- SANCER, M. I., 'An Analysis of the Vector Kirchhoff Equations and the Associated Boundary Line Charge', *Radio Science*, vol. 3, pp. 141-144, 1968.
- SCHANDA, E., 'Physical Fundamentals of Remote Sensing', Berlin, 1986.
- SCHEFFER, F. & SCHACHTSCHABEL, P., 'Lehrbuch der Bodenkunde', 13. durchgesehene Aufl. von P. Schachtschabel, H.-P. Blume, G. Brümmer, K.-H. Hartge und U. Schwertmann, Enke Verlag, pp. 491, 1992.
- SCHULER, D. AINSWORTH, T., LEE, J. S. & DE GRANDI, G., 'Topographic Mapping Using Polarimetric SAR data', *International Journal of Remote Sensing*, vol. 34, no. 5, pp. 1266-1277, 1998
- SHEPARD, M. K, BRACKETT, R. A. & ARVIDSON, E., 'Self-affine (fractal) topography: surface parametrization and radar scattering', *J. of Geophy. Res.*, vol. 100, no. E6, pp. 11, pp.709-11,718, 1995.
- SHI, J., WANG, J., HSU, A. Y., O'NEILL, P. E. & ENGMAN, E., 'Estimation of Bare Surface Soil Moisture and Surface Roughness Parameters Using L-band SAR Image Data', *IEEE Transactions on Geoscience and Remote Sensing*, vol. 35, no. 5, pp. 1254-1264, 1997.
- SHIN, T. R. & KONG, J. A., 'A backscatter model for a randomly pertubated periodic surface', *IEEE Transactions on Geoscience and Remote Sensing*, vol. 20, no. 4, 1982.
- SHIVOLA, A, 'Properties of dielectric mixtures with layered spherical inclusions', in: *Microwave Radiometry and Remote Sensing Applications*, ed. P. Pampaloni (Utrecht, VSP), pp. 115 – 123, 1989.
- SILVER, S., 'Microwave Antenna Theory and Design', McGraw-Hill Book Company, New York, 1947.
- STACHEDER, M., 'Die Time Domain Reflectometry in der Geotechnik: Messung von Wassergehalt elektrischer Leitfähigkeit und Stofftransport', *Schr. Angew. Geol. Karlsruhe*, vol. 40, I – XV, pp 170, 1996.
- STRATTON, J. A., 'Electromagnetic Theory', McGraw-Hill Book Company, New York, 1941.
- TOPP, G. C., DAVIS, J. L., & ANNAN, A. P., 'Electromagnetic Determination of soil water content: Measurements in Coaxial Transmission Lines', *Water Resour Res.*, vol. 16, no. 3, pp. 574 – 582, 1980.
- ULABY, F, MOORE, R., & FUNG, A., 'Microwave Remote Sensing: Active and Passive I – III', Addison-Wesley Publication, pp. 2162, 1981-1986.
- VON HIPPEL, A., 'Dielectrics and Waves', vol. I and II, pp. 284, 1954, reprint 1995.
- WHALLEY, W. R., 'Considerations on the use of time domaine reflectometry (TDR) for measuring soil water content', *J. Soil. Sci.*, vol. 44, pp. 1 – 9, 1993.

ZRIBI, M., CIARLETTI, V. & VIDAL-MADJAR, D., 'An Inversion Model of Soil Roughness Based on Two Radar Frequency Measurements', Proceedings IGARSS'99, Hamburg, pp. 2425 - 2427, 1999.